Simulation and Experiments of Mixing and Segregation in a Tote Blender

O. S. Sudah, P. E. Arratia, A. Alexander, and F. J. Muzzio
Dept. of Chemical and Biochemical Engineering,
Rutgers University, Piscataway, NJ 08855

DOI 10.1002/aic.10448
Published online in Wiley InterScience (www.interscience.wiley.com).

Experimental and computational investigation of mixing and segregation of granular material in a tote blender was carried out. The discrete element method (DEM) was used to simulate flow of spherical, free-flowing particles where the results of the computations were compared to blending. Computational results are compared to blending experiments of monodisperse and bidisperse systems using spherical glass beads in a 1:1 scale. Although some discrepancies were observed, DEM simulations illustrated good agreement with experimentally measured mixing and segregation rates for different fill levels and loading conditions. The effects of blender geometry on particle velocities and flow patterns were examined using DEM. The presence of a hopper and bin section, as well as the axial offset proved to introduce greater axial mixing rates that would be expected from pure dispersion. Vibrated experiments showed better agreement than not-vibrated experiments, indicating that modeling of friction forces needs to be further improved to enhance the accuracy of DEM methods. © 2005 American Institute of Chemical Engineers *AIChE J,* 51: 836–844, 2005
Keywords: tote blender, powder mixing, granular blending, DEM, particle dynamics

Introduction

Particles are an integral part of our natural environment and are a major component in many manufacturing operations in the production of pharmaceuticals, foodstuffs, polymers, and consumer goods. Final product quality can be critically affected by the ability to create homogeneous blends of powders and granules. For example, ineffective blending of pharmaceutical products can result in dangerous variability of active concentrations in tablets and capsules. These concentration variabilities can have serious consequences on product efficacy and safety. However, the characterization of mixing and flow of granular materials in industrial blenders remains underdeveloped due to inefficient sampling methods, difficulties with gathering relevant experimental data, and poorly-defined material properties. As a result, design and scale-up of blending equipment and operations is largely *ad hoc*.

One rapidly growing avenue for the study of blending and flow of granular materials in tumbling blenders is computer simulations. Validated computer simulations provide data that would be very difficult to extract from experimental systems, such as information on stress, strain, voidage, and velocity distributions. Furthermore, simulations can be used to perform parametric studies for equipment prototypes prior to construction (Sudah et al., 2002). However, despite their usefulness, 3-D particle simulation studies using industrially relevant blenders are scarce in the literature (Moakher et al., 2000).

Background

Granular flow models are typically divided into continuum and discrete models. Continuum models neglect the discrete nature of particles and assume that the granular material is a continuum that obeys mass and momentum conservation laws (Goodman and Cowin, 1972). Discrete models, on the other hand, treat each particle as a distinct entity, and offer two

Correspondence concerning this article should be addressed to F. J. Muzzio at muzzio@soemail.rutgers.edu

primary advantages: (1) no *a priori* assumptions are needed regarding the state of bulk microstructure, and (2) individual particle properties (size, shape, elasticity, surface roughness, and so on) can be used as direct inputs into the models. Discrete models can be subdivided into many classes, including Kinetic theory models that treat granular systems as ensembles of interacting and colliding gas molecules (Chapman, 1970), Monte Carlo methods that apply probabilistic rules (Rosato et al., 1986; Hopkins and Shen, 1992), cellular automata that apply deterministic rules (Jullien et al., 1992; Yanagita, 1999), and particle dynamics methods that derived rules from first principles (Walton, 1983).

Two types of particle dynamics methods are most common: "hard-particle" methods, in which collisions are instantaneous and binary, and "soft-particle" methods in which collisions can be lasting and may involve more than two particles. Typically, hard-particle methods are most useful in rapid granular flows, where collisions are discrete and distinct. Inelastic collapse (Shinbrot and Muzzio, 2000) is a limitation of the hard particle method, where the time between collisions of two objects approaches zero as they become closer to each other (for example, ball bouncing on a flat surface), hence, the time step for calculation becomes equal to zero for enduring contacts. Therefore, hard particle methods are not useful for modeling granular systems whose particles are in continuous contact. Under these conditions, soft particle methods, which permit minute deformation of particles, are more appropriate. The soft-particle approach is appropriate for studying flow in tumbling blenders, which is characterized by long contact times between particles.

A commonly used particle dynamics method for the modeling of granular flow is the discrete element method (DEM). DEM uses Newtonian physics to determine the velocity, angular momentum, and position of particles. Each particle is tracked in the system and particle-particle and particle-boundary interactions are computed. DEM simulations are often thought of as a macroscopic equivalent of short-range molecular dynamics in which the inelastic nature of particle collisions is taken into account (Sawley and Cleary, 1999). In recent years, the use of particle dynamic simulations has proliferated (Walton, 1983; Walton and Braun, 1986; McNamara and Young, 1992; Luding et al., 1994; Ristow, 1996; Bizon et al., 1998), and currently is being applied toward solving complex industrial problems (Cleary and Sawley, 1999; Pfeffer et al., 2001).

In this article, we apply 3-D DEM to study flow and mixing of spherical, free-flowing particles in a 14L tote blender. This approach is currently limited in particle numbers to O(104), which is far fewer than the number of particles in any real application, but has been shown to give reasonable results for free-flowing materials (Moakher et al., 2000). The computational work was validated using glass beads in 1:1 scale experiments that allow qualitative and quantitative comparison of mixing and segregation in these systems. The goal of this investigation was to examine the feasibility of using particle dynamics simulation to predict blending performance in industrial type blenders with the aim of expanding the range of available tools currently limited to experimental methods. Herein, the vessels were small and the particles were large in comparison to real applications, which limits our ability to make direct correlations to larger systems. The major benefit

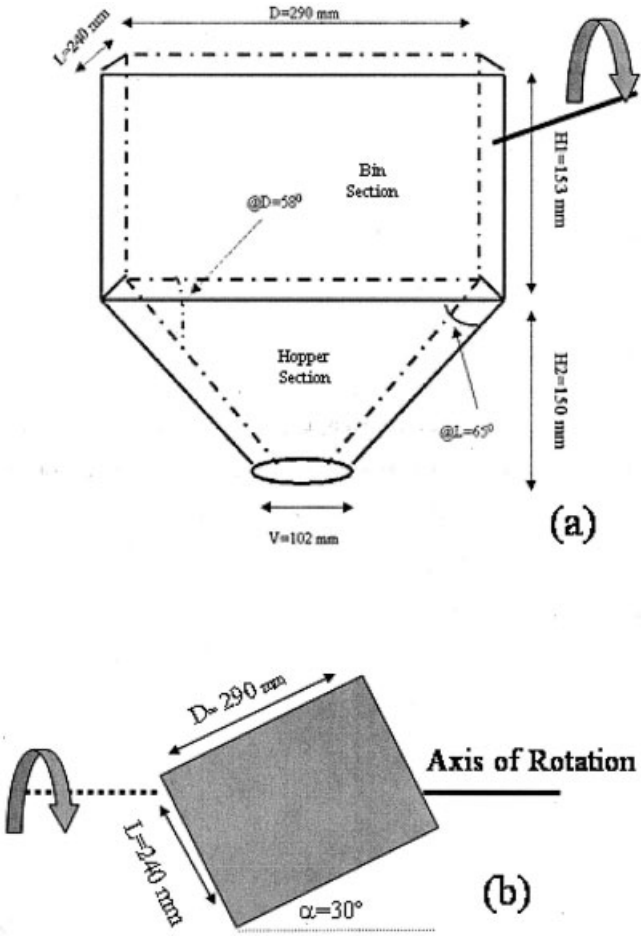

Figure 1. (a) Dimensions of the GEA Gallay tote blender used for simulation and experiments, and (b) Top view and axis of rotation.

was that the motions of individual particles can be tracked, and this information can be useful in understanding the mixing and segregation mechanisms within the blender. It is currently impossible to determine whether these mechanistic explanations will scale-up properly and only by comparing to results from "real" systems can the utility of these mechanistic descriptions be evaluated.

Material and Equipment

We carried out the blending experiments in a 14-L GEI Gallay tote blender that was geometrically analogous to full-scale blenders employed in pharmaceutical manufacturing facilities. The geometry and dimensions of the blender are shown in Figure 1a. The axis of rotation passes through the center of the blender but was offset by 30° to mirror the design of larger blenders (Figure 1b). Black and white glass beads of 6 mm and 12 mm dia. were used in this study (JB Import and Export LLC, Franklin, NJ).

Methods

Sampling

Once the blender had been rotated for the desired number of revolutions, it was dismounted from the drive and the bed was

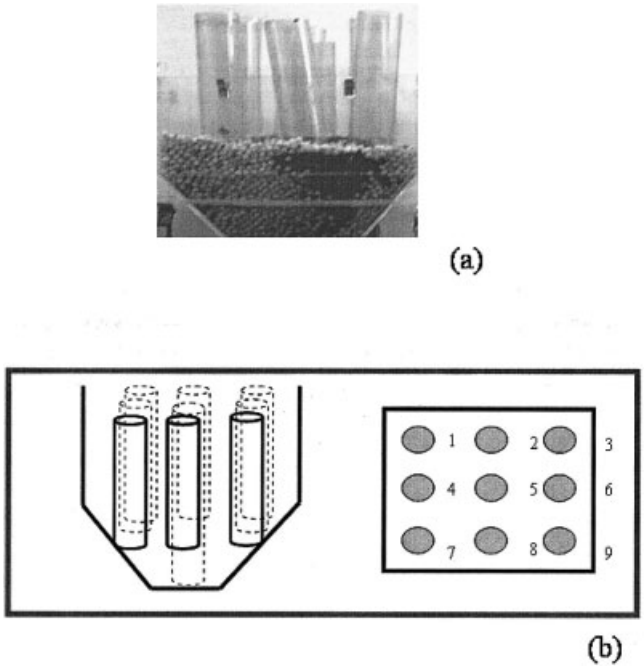

Figure 2. Sampling: (a) sampling procedure, and (b) experimental sampling scheme and the location of the nine cores used to quantify concentration.

sampled using large transparent core samplers (Muzzio et al. 1997). For this system, the core samplers were plastic tubes (3/4 in. outer dia., 11/16 in. inner dia. that spanned the cross section of the blender as illustrated in Figure 2. Nine core samplers were inserted into the mixture; the sampling scheme is shown in Figure 2b. Once in place, a transparent tube slightly smaller in diameter than the core samplers was inserted into the core samplers one at a time. The tube was fitted with a screen mesh that prevented particles from exiting the top of the tube. After the tube was inserted, vacuum was applied, trapping the beads in the tube. The tube was then removed, vacuum deactivated, and the beads were discharged into a sample collection cup. This method prevented preferential vacuuming of small beads over larger ones and generated nine core samples per experimental timepoint. Core sampling has been shown to give much more reproducible and accurate concentration information than other sampling methods (Muzzio et al. 1997, 2002). The samples were analyzed by separating the beads and weighing them to obtain concentration data. This procedure retrieved 9 samples per time point however the large size of the samples and complete coverage of the blender volume provide a reasonable measure of mixture concentration. Upon completion of an experiment, all the beads were separated and loaded anew in the tote blender. Hence, each experimental time point represents a completely new experiment.

DEM Simulations

The model employed in this communication considers granular material as a collection of frictional, partially elastic spherical particles. Each particle may interact with its neighbors or with the boundary of the blender through both normal and tangential forces. The elastic modulus and computational timestep are chosen so that deformations of particles remain small when compared with their displacements and diameters. The normal forces that develop between particles in contact are calculated using the "partially latching spring" model of Walton and Braun (Walton and Braun, 1986). This model approximates the elastic-plastic behavior of contracting spheres observed in laboratory experiments and in finite element calculations. The normal forces F_{ij}^n, acting on particle i with position vector r_i, and radius R_i, resulting from its interaction with particle j, with position vector r_i, and radius R_i, is taken to be the following function of the overlap for loading and unloading, respectively

$$\alpha_{ij} = |r_i - r_j| - (R_i - R_j) \tag{1}$$

$$F_{ij}^n = \begin{cases} K_1 \alpha_{ij} n_{ij} & \text{if } \alpha_{ij} \geq 0 \text{ (loading)} \\ K_2(\alpha_{ij} - \alpha_o) n_{ij} & \text{if } \alpha_{ij} < 0 \text{ (unloading)} \end{cases} \tag{2}$$

$$n_{ij} = \frac{(r_i - r_j)}{|r_i - r_j|} \tag{3}$$

where *nij* is the unit vector joining the centers of the two particles, and K1 and K2 are the normal stiffness coefficients for loading and unloading, respectively. The stiffness coefficient for unloading is taken to be larger than that of loading (Walton, 1993). For simple binary collisions, this model produces a coefficient of restitution

$$\varepsilon = \sqrt{\frac{K_1}{K_2}}, \tag{4}$$

that is independent of the relative velocity of impact. Tangential forces are calculated using Walton's 3-D "incrementally slipping" model (Walton, 1993). After contact occurs, static frictional force builds up nonlinearly with displacements in the tangent plane of contact. Once a threshold of maximum static frictional forces is reached, bodies slide with constant dynamic friction coefficient.

Particle interactions were tracked using linked list algorithms described elsewhere (Moakher et al., 2000) and the resulting equations of motion were integrated using a "leapfrog" algorithm. The equations of motions are written as a system of two sets of ordinary differential equations: one for positions and the other for velocities. The latter is integrated first then the former and the acceleration is evaluated for the next time step. Particles in a tumbling blender can be in relative motion with respect to the blender's boundary, which in turn rotates with respect to a fixed frame. To simulate particle motions within vessels undergoing a general rotational motion (not necessarily a simple rotation about a fixed axis), it is useful to write the equations of motion in a frame attached to the vessel. The advantage of this choice is that contact detection between particles and the blenders' inner wall, and computation of the resulting particle-wall forces, is considerably simplified. This overall model scheme has two advantages: (1) it approximates the elastic-plastic behavior of contacting spheres observed in laboratory experiments (Hopkins and Shen, 1992), and (2) it accurately reproduces the experimentally observed

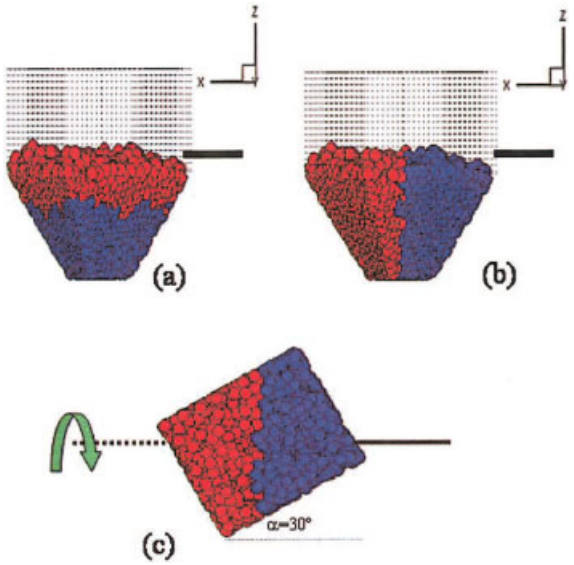

Figure 3. Initial conditions for monodisperse simulation and experiments: (a) top-bottom, and (b) left/right loaded cases, and (c) axis of rotation.

flow behavior of particles in the V and double cone blenders (Moakher et al., 2000).

Blending and Computational Experiments

Two types of experiments were performed in this investigation: (1) monodisperse, where the all the beads were 12-mm in dia. differing only in color, and (2) bidisperse, where half of the beads (by volume) were 12-mm in dia. and the rest 6-mm in dia. All experiments were performed at 10 RPM.

For the monodisperse case, the material was initially loaded into the tote blender in one of two ways, top-bottom loading or left/right loading. Top-bottom loading was achieved by pouring the first component into the blender, leveling, then pouring in the other component. Left/right loading was achieved by first inserting a cardboard separator perpendicular to the axis of rotation dividing the blender into two halves that were filled with a single-color bead. Once loaded, the divider was carefully removed, leaving the division plane between the two components perpendicular to the axis of rotation. The bidisperse case, on the other hand, had a different initial loading condition. Equal amounts of 12-mm and 6-mm beads were hand mixed together to attain a visually homogeneous system, and then loaded into the tote blender using a scoop (free flow of the beads was avoided to minimize segregation prior to blender rotation).

Consistent with the goal indicated in the introduction, the vessel used in the computational work was configured to have the same dimensions as the actual vessel used in the laboratory experiment. Particle size was chosen to obtain a 1:1 relation with experiments. While this approach necessitated large particle sizes, the simulation was limited by the number of particles used for a reasonable number of vessel rotations. In addition, for small particles, other forces that are not included in our model scheme, such as electrostatic forces, become relevant, compromising the accuracy of the DEM model in its current state of development.

For monodisperse mixtures, two fill percentages were simulated, 40% fill (3,700 particles) and 60% fill (5,500 particles). For each fill level, two types of initial loading patterns were analyzed: top-bottom and left/right loading patterns as shown in Figure 3a and 3b, respectively. The angle of the axis of rotation (30°) was taken into account as shown in Figure 3c. Simulations for the bidisperse case were performed at 40% fill, consisting of 1833 12mm beads and 14666 6mm beads (quantities chosen to produce nearly equal volumes of each material). The bidisperse system had the particles initially placed in a random order prior to blending. All simulations were performed at 10 RPM.

The simulation output data were quantified by numerically sampling the mixture at different time points by dividing the spatial domain of the system into cubic boxes. Boxes overlapping the tote boundaries were not considered, and a 12-particle threshold was placed on the number of particles in each sample box, below which the box is discarded. The average sample size was 30 particles for the monodisperse simulation, and 100 particles for the bidisperse simulation.

Results

Mixing rates

Prior studies of mixing and segregation in tumbling blenders have suggested that blenders with reflectional symmetry suffer hindered transport across the symmetry plane. The blender under consideration here, even though geometrically symmetric, rotates on an axis that is 30° offset from the symmetry plane (Figure 3c). The offset axis copies the rotation axis used for larger blenders with the same geometry and was intended to improve axial transport across the mid-plane, which is usually the rate-limiting factor in achieving homogeneous mixing.

The difference between axial and radial mixing rates is qualitatively demonstrated in Figure 4, which shows the evolution of mixture concentrations for 40% fill when particles are separated in a top/bottom (Figures 4(a–d)) and left/right (Figures 4(e–f)) manner. Initial conditions are shown as an insert in Figure 4a and Figure 4e. We can readily see that while the top-bottom case is nearly completely homogenized by the convective mixing process after only 8 revolutions, the left/

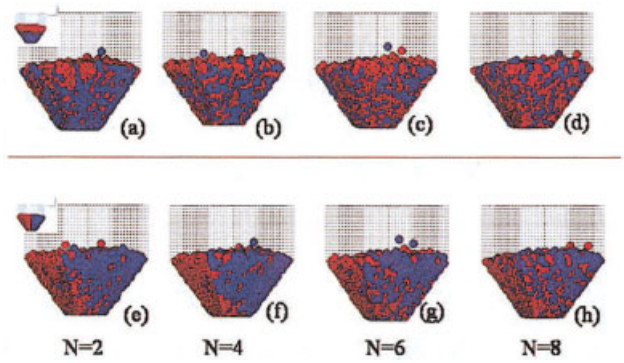

Figure 4. Monodisperse and bidisperse experiments and simulations at 60% fill for (a,e) 2 revolutions, (b,f) 4 revolutions, (c,g) 6 revolutions and (d,h) 8 revolutions.

Inserts correspond to initial conditions.

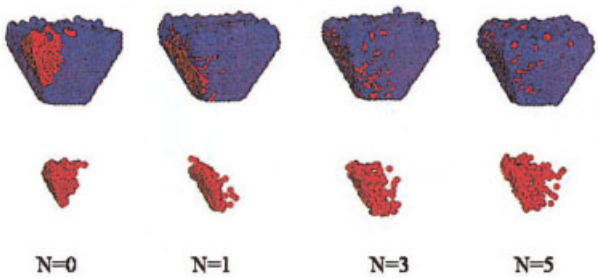

Figure 5. Dispersion experiments for a 40% fill level case.

right case is still far from homogeneous, indicating a much slower mixing process. To further illustrate this point, we initially load red particles in the upper left corner of the blender as shown in Figure 5 for a 40% fill level case and followed particles for 5 revolutions. The simulations revealed that particles appeared to be uniformly "mixed"within the left half of the blender, but very little transport was evident between the two halves of the blender. By blanking the blue particles and just concentrating on the red particles, it was observed that the red particles slowly mixed along the axis of rotation. The above simulation experiments illustrated that, despite the asymmetric axis of rotation, axial mixing from particle transport parallel to the axis of rotation remained a slow process compared to radial mixing perpendicular to the axis of rotation.

Mixing curves were constructed by plotting the relative standard deviation (RSD) vs. mixing time. The relative standard deviation (a.k.a. coefficient of variability) is calculated as

$$RSD = \frac{\sigma}{\bar{C}}, \tag{5}$$

where

$$\sigma = \sqrt{\frac{\sum_{i=1}^{N} (\bar{C} - C_i)^2}{N - 1}}, \tag{6}$$

N is the total number of samples in one experiment, $\bar{C}$ is the theoretical average concentration, and C_i is the sample concentration.

Figure 6 compares mixing rates for experiments and simulations by plotting the decrease in RSD vs the number of revolutions for 40% fill, top-bottom and left/right initial conditions. The mixing curves for the left/right cases in Figure 6 are in very good agreement both qualitatively and quantitatively. The mixing curves for the 40% fill top-bottom loaded case collapse at longer time, however, the experiments mix faster than the simulations at short time. Previous work by Shinbrot (Shinbrot et al., 1999) has shown that increased friction can increase the axial mixing rate. In this case, it is possible that the simulations do not account for friction between particles thus leading to decreased mixing rates. Further experiments were undertaken in which the entire blender assembly was vertically vibrated at 10 Hz with an acceleration of 0.6 g (6 cm-amplitude peak to peak) during vessel rotation. The vibration of the vessel during rotation was intended to reduce

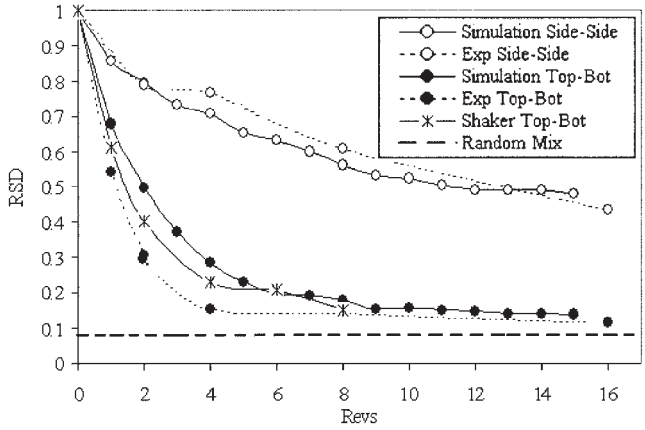

Figure 6. Mixing curves for 40% fill monodisperse case initially loaded left/right (open circles), top-bottom (closed circles), and vertically vibrated experiments (asterisks).

Dashed line represents experiments, and solid lines represent simulation results.

particle-particle friction in the experiments, which may improve the agreement with simulations. The results from the vibrated experiments are plotted as asterisks in Figure 6, and show better agreement with the simulations results than the nonvibrated experiments. This agreement indicates that the friction modeling used in the simulations is not very predictive for radial mixing rate which is sensitive to mixture frictional effects.

Figure 7 shows RSD vs the number of revolutions for 60% fill, top-bottom and left/right initial loading patterns for the simulations and experiments. Similar to the results for 40% fill, experiments and simulation show very good agreement for left/right loading at 60% fill. For top/bottom loading, agreement is better than that seen for 40% fill, although the experiments again show faster mixing rates at very short times. The data from Figures 6 and 7 indicate that simulations adequately

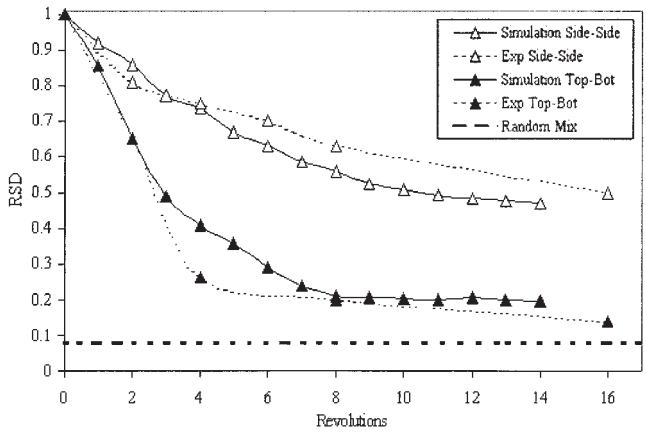

Figure 7. Mixing curves for 60% fill monodisperse case initially loaded left/right (open triangular symbols) and top-bottom (closed triangular symbols).

Dashed lines represent experimental data, and solid lines represent simulation data.

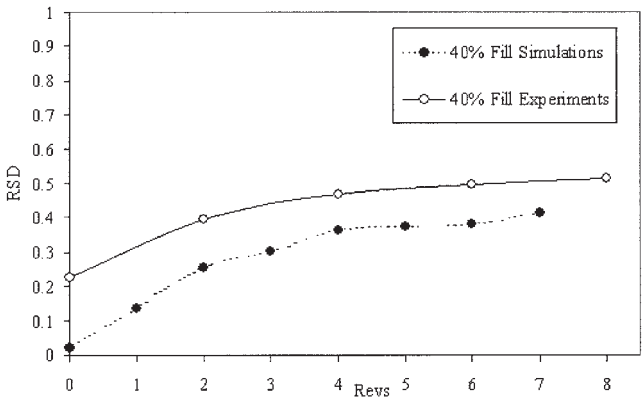

Figure 8. Segregation curve for the bidisperse mixture at 40% fill (circular symbols).

Dashed lines represent the simulation data, and solid lines represent experimental data.

predict axial mixing rates, however, miss some specifics relating to radial mixing rates.

Close examination of the simulation results for both fill levels, shows that for left/right loading, there was virtually no difference in mixing rates, however, for top/bottom had a consistent gap between the 40% data and the 60% data. For left/right loading, axial mixing is the dominant mechanism and is primarily dependent on the dispersion of particles on the surface of the mixture. Changes in fill level from 40% to 60% do not substantially change the surface area or shape of the flowing surface and little change in axial mixing rate is expected (at very low or high fill levels, for example, 20 and 80%, axial mixing invariance rate may no longer hold true). In contrast, mixing mechanisms for top/bottom loading are dependent on iterative striation formation (Shinbrot et al., 1999), and changes in fill level can have significant impacts on the radial mixing rate. A more complete description and comparison of axial and radial mixing for free-flowing materials in tote-blenders can be found in (Alexander et al., 2004).

Segregation

Figure 8 displays the RSD of the smaller 6mm particles as a function of the number of revolutions for the bidisperse case for both the simulations and the experiments at 40% fill. The initial state was different for the experiments and the simulation. The computer is able to more fully randomize the mixture than can be achieved in the laboratory, as is evident from the difference in RSD values at zero time. Due to the different initial "mixed" states, it is more useful to make a comparison of the results by considering the rate of segregation for each case, rather than the proximity of the data. It has been previously suggested in the literature (Zik et al., 1994; Cantelaube et al., 1997; Choo et al., 1997) that segregation maybe described by first-order kinetics, where the intensity of segregation increases exponentially with time according to

$$RSD_{asympt} - RSD = Be^{-SN} \tag{7}$$

where S is the rate of segregation constant, B is a constant pre-factor, N is the number of revolutions and RSDasympt is the observed asymptotic RSD.

Taking the natural log of Eq. 3, and linearly regressing it to the data in Figure 8, parameters B and S were estimated. The values of S for 40% fill level bidisperse case were estimated to be 0.34 and 0.28 for simulations and experiments, respectively. This acceptable agreement between experiments and simulations indicate that the model is able to adequately capture the overall segregation rate at short time. However, these are short term results and stronger segregation patterns have shown to form in other tumbling blenders at longer times, and may be applicable to this system at longer periods.

Velocity Fields and Flow Mechanism

A great advantage of computational models is that one can easily extract useful information that would be difficult to obtain experimentally. For instance, velocity profiles in the cascading layer can be easily obtained. Figure 9 shows a snapshot of the velocity field at 3/4 of a rotation cycle at 60% fill (0 is the upright position (Figure 1) indicating a thin high velocity flowing layer atop a slow moving region below. This is in agreement with the current understanding of flow in a tumbling blender: a thin, rapid flow region near the surface, a near nondeforming region beneath that rotates with the tumbler as a solid body, and a narrow transition region between characterized by high-shear and density gradients. The rapid layer is a flat, thin region of 2 to 3 particle diameters, which remains nearly constant in size for the fill levels discussed here. Examination of changes in the size or shape of the flowing layer with variations in fill level or rotation rate is beyond the scope of this article. Examination of the velocity profiles in the cascading region can yield information about mixing mechanisms that would be difficult or impossible to gather from experimental observation.

Typically, axial mixing in tumbling blenders has been shown to be orders of magnitude slower than radial mixing. For perfectly symmetric blenders, such as cylinders or double cone blenders, dispersion is most likely the dominant mechanism because there are no mechanisms for imparting axial flow. The tote-blender discussed in this communication is a symmetric blender, but it is rotated 30% offset from the symmetry plane, which functionally renders it an asymmetric blender. This

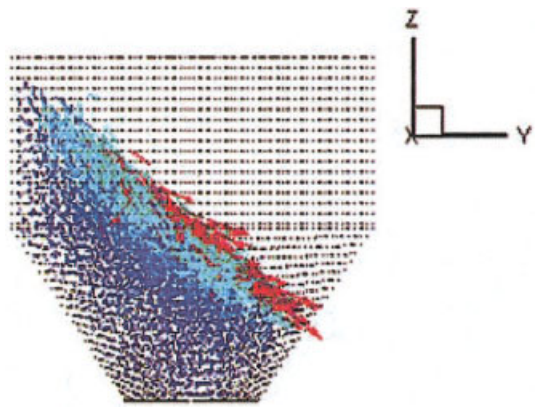

Figure 9. Velocity vectors for a monodisperse 60% fill level case at 3/4 of a turn.

A vertical line at 0 cm/s highlights the differences in leftward and rightward movement.

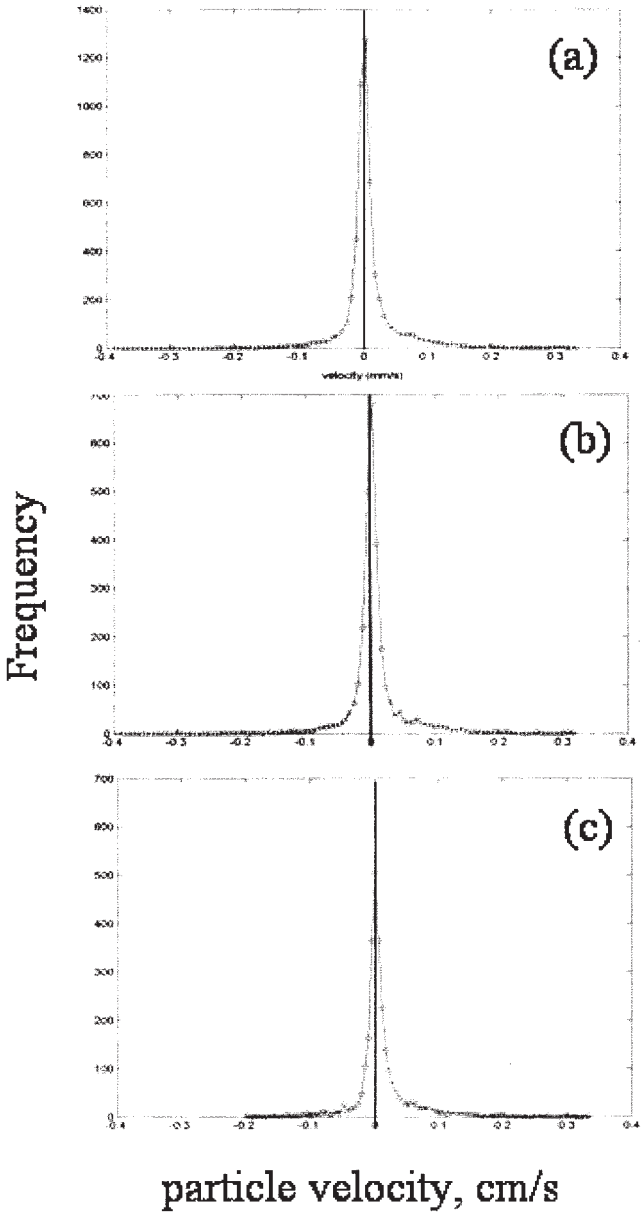

Figure 10. Probability density function (pdf) of axial velocities of a monodisperse 60% fill level case: (a) all particles, (b) particles located in the left side of the blender (−x), and (c) particles located in right side of the blender (+x).

asymmetry creates axial flows in the blender that help to greatly increase the axial mixing rate when compared to pure dispersive mixing rates.

We examine the effects of blender geometry on particle velocities in the axial direction by extracting particle velocities parallel to the axis of rotation at specific snapshots in time. In Figure 10a, we show the probability density function (pdf) of axial velocities when the blender has turned 1/16 of a revolution at 60% fill. The average axial velocity at this blender orientation is 0.0083 cm/s in the positive direction (to the right), which is small compared to the average "downhill" velocity in the cascade (~0.3 cm/s) but significant. We can also examine the probability density function (pdf) for axial velocity on the right and left halves of the blender (Figure 10 b,c), which show similar characteristics and both indicate a general flow to the right (-0.0034 cm/s for the left half and 0.006 cm/s for the right half). In a true dispersive flow, the average axial velocity should be zero because the probability of "dispersing" should be equivalent in both directions. Table 1 shows the average axial velocity at consecutive blender positions during a single rotation, using 0 as the upright state.

The velocities in Table 1 indicate that axial flow in the tote-blender changes direction from right to left and back as the blender undergoes one complete revolution. This inherent axial flow increases axial mixing rates when compared to expected mixing rates for pure dispersive mixing. A 56 L tote-blender (~48 cm in width) has been shown to take more than 240 revolutions to reach suitable RSD values when mixing 400-micron sand (Alexander et al. 2001), comparatively, it took upward of 1,000 revolutions to mix 60-micron glass beads loaded side-by-side in a 14 cm long rotating cylinder (Wightman et al. 1998). Clearly, adding a minor axial flow component during blender rotation can have an enormous impact on axial mixing rates.

During blender rotation, axial flows develop because the mixture in the blender does not flow in a geometrically symmetric environment. Close to the upright position, the mixture flows toward a wall that is sloped to the right, which causes the entire mixture to flow rightward. Similarly, in the inverted position, flow is toward a leftward slanting wall, causing flow leftward. Previous experiments with a salt (potassium chloride, KCl) and microcrystalline cellulose (MCC) mixture provided evidence of these flow biases. A 56L tote-blender was loaded to 60% of capacity by adding MCC (PH102 Avicel) first and then KCl on top. Figure 11 shows the measured concentrations of core samples taken from the blender with increasing revolutions.

It is important to repeat that experiments were run using a top/bottom axially symmetric loading condition. Figure 11 and Table 2 indicate a large-scale movement of the salt particles from left-to-right early in the mixing process. Apparently, in the initial stages of the first revolution of the blender, as the mixture flowed toward the sloped wall, the free-flowing salt, which was the upper layer of the mixture, moved rightward. Later in the first revolution flow to the left did not "reverse" this initial shifting because the portion of the mixture that is in motion as it flows toward the leftward wall is not necessarily composed of mostly salt. Further revolutions of the blender did not significantly move the salt back to the left because radial

Table 1. Average Partial Axial Velocities for 60% Fill Level Case at Different Blender Position

Blender Position	Average Axial Velocity (cm/s)
1/16	0.0083
1/8	0.0144
1/4	0.0051
3/8	−0.0075
1/2	−0.006
5/8	−0.011
3/4	−0.0055
7/8	0.0085
15/16	0.0083

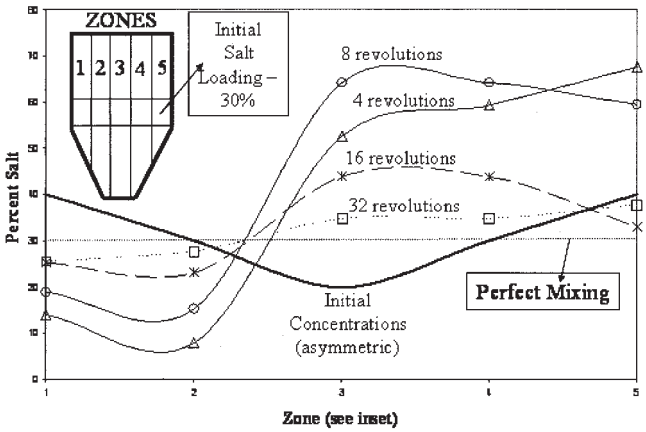

Figure 11. The change in salt concentration with increasing revolutions for a 56 L tote-blender loaded with 30% salt at 60% fill.

The initial concentration line is approximated and asymmetric because the relative initial amounts of salt in each zone is not constant.

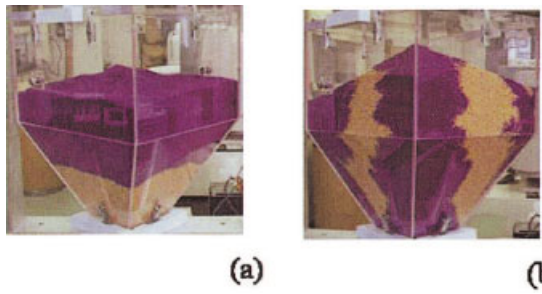

Figure 12. 1.8mm (gold) and 0.6mm (purple) particles segregate at 10 rpm (60% fill level).

(a) Initial condition, and (b) after 64 revolutions.

mixing decreased the free-flowing nature of the salt by diluting it with MCC. As the blender rotated further, the mixture slowly mixed axially and resulted in a well-mixed state after ~128 revolutions, for pure radial mixing, a well-mixed state would be expected in ~50 revolutions or less.

Perhaps, the most interesting flow patterns occurred when the mixture flowed into or out of the hopper section (Figure 1). As the mixture flows from the hopper section into the bin section, particles on either side of the mixture diverge as the bin section is filled. The simulations captured these flows - at 1/4 turn, axial velocities in the left half of the blender were -0.0028 cm/s, while in the right half they were 0.019 cm/s. Thus, particles in the left half drifted left and in the right half drifted right. The opposite situation arised when the mixture flowed from the bin section into the hopper section. At 13/16 turn, flow in left half was 0.0053 cm/s and in the right half it was -0.014 cm/s - particles were converging. Similar flow patterns have been shown to lead to the formation of segregation patterns for bidisperse mixtures in double cone blenders (Alexander et al., 2001). Similar segregation patterns have been noted in a tote-blender run at 10 rpm, a mixture of 1.8 mm and 0.6 mm particles formed a stable segregation pattern, as shown in Figure 12. In this case, a balance is maintained between rightward and leftward flow in each half of the blender, leading to a striped pattern.

Conclusions

A qualitative and quantitative experimental validation of particle dynamics simulation in fully 3-D tote blenders was presented. For most cases, good agreement between particle dynamics simulation and the experimental results was obtained for the mixing and segregation of free flowing particles in tote blenders. The particle dynamics model not only captured particle behavior and shape of mixing/segregation curves as a function of fill and loading pattern, it also predicted the measured degree of mixing and segregation for most of the experiments performed. The observation that convective mixing was faster in experiments than in simulations at short mixing time can be attributed to the fact that not all friction forces are properly accounted for by the soft particle dynamics model used here. This likely resulted in a smaller shear layer in the simulations, producing a lower RSD value at short time (2-4 revolutions).

We investigated the effects of blender geometry on particle velocities and flow patterns. The presence of a hopper and bin section, as well as the axial offset proved to introduce greater axial mixing rates that would be expected from pure dispersion. The imparted axial flow changed direction as the blender rotated, increasing particle movements in the axial direction, and, hence, increasing the axial mixing rate. This flow bias was also detected in a larger, geometrically similar blender using a salt/MCC mixture. In addition, we are able to capture a converging and diverging flow mechanism when particles flow from bin to hopper and from hopper-to-bin, respectively. This flow mechanism is most likely responsible for the segregating patterns observed in long-term experiments with other particle sizes; similar flow mechanisms have been shown to lead to formation of segregating patterns in double cone blenders.

Overall, 3-D DEM simulations proved to be a valuable tool to investigate mixing and segregation in tumbling blenders. The wealth of data that can be obtained from simulations can be used to explain many phenomena observed during experiments.

Table 2. Salt Concentration in a 56L Gallay Tote Blender

Salt Concentration From Left-to-Right (% By Weight)					
Revolutions	Leftmost	Left	Center	Right	Rightmost
4	13.9	7.8	52.6	59.3	67.6
8	18.9	15.2	64.2	64.2	59.5
16	25.3	23	42.8	43.8	33
32	25.6	27.6	34.6	34.6	37.6

Acknowledgment

This work was supported by grants from Torpharm (Ontario Canada) and GEI Gallay Systems Ltd. (Birmingham, UK).

Literature Cited

Alexander, A., and F. Muzzio, et al.. "Effects of Scale and Inertia on Granular Banding Segregation," *Granular Matter,* **5**(4), 171 (2004).

Alexander, A., and T. Shinbrot, et al.. "Granular Segregation in the Double-Cone Blender: Transitions and Mechanisms," *Phys. Fluids,* **13**(3), 578 (2001).

Bizon, C., and M. D. Shattuck, et al.. "Patterns in 3D Vertically Oscillated

Granular Layers: Simulation and Experiment," *Phy. Rev. Lett*., **80**(1), 57 (1998).
Cantelaube, F., and D. Bideau, et al.. "Kinetics of Segregation of Granular Media in a Two-Dimensional Rotating Drum." *Powder Tech*., **93**,1 (1997).
Chapman, S., T. G. Cowling, The Mathematical Theory of Non-Uniform Gases, 3rd ed. Cambridge, Cambridge, UK (1970).
Choo, K., T. C. A. Molteno, et al. "Traveling Granular Segregation Patterns in a Long Drum Mixer," *Phy. Rev. Lett*., **79**(16), 2975 (1997).
Cleary, P. W. and M. L. Sawley. DEM Modelling of Industrial Granular Flows: 3D Case Studies and the Effect of Particle Shape on Hopper Discharge. *2nd Int. Conf. on CFD in the Minerals and Process Industries* CSIRO, Elsevier, Australia (1999).
Goodman, M. A. and S. C. Cowin, "A Continuum Theory for Granular Materials. Arch," *Rational Mech. Anal.,* **44**, 249 (1972).
Hopkins, M. A. and H. H. Shen, "A Monte Carlo Solution for Rapidly Shearing Granular Flows Based on the Kinetic Theory of Dense Gases," *J. of Fluid Mech*. **244**, 477 (1992).
Jullien, R., P. Meakin, et al., "Three-Dimensional Model of Particle-Size Segregation by Shaking," *Phy. Rev. Lett*. **69**(4), 640 (1992).
Luding, S., E. Clément, et al. Onset of Convection in Molecular Dynamics Simulations of Grains. *Phy. Rev. E.,* **50**(3), R1762–R1765 (1994).
McNamara, S. and W. R. Young, "Inelastic Collapse and Clumping in a One-Dimensional Granular Medium," *Phys. Fluids,* **4**(3) 496 (1992).
Moakher, M., T. Shinbrot, et al.. "Experimentally Validated Computations of Flow, Mixing and Segregation of Non-Cohesive Grains in 3D Tumbling Blenders, *Powder Tech*., **109**, 58 (2000).
Muzzio, F., C. L. Goodridge, et al.. Sampling and Characterization of Pharmaceutical Powders and Granular Blends. *Int. J. of Pharmaceutics*, **250**(1), 51 (2002).
Muzzio, F. J., P. Robinson, et al.. "Sampling Practices in Powder Blending," *Int. J. Pharm.*, **155**,153 (1997).
Pfeffer, R., R. N. Dave, et al.. "Synthesis of Engineered Particulates with Tailored Properties using Dry Particle Coating," *Powder Tech*., **117**(1-2), 40 (2001).
Ristow, G. H. "Dynamics of Granular Materials in a Rotating Drum," *Europhysics Lett*., **34**(4), 263 (1996).
Rosato, A., F. Prinz, et al.. "Monte Carlo Simulation of Particle Matter Segregation," *Powder Technol*., **49**,59 (1986).
Sawley, M. L., and P. W. Cleary, "A Parallel Discrete Element Method for Industrial Granular Flow Simulations," *EPFL Supercomputing Revie,*. **11**, 23 (1999).
Shinbrot, T., A. Alexander, et al.. "Chaotic Granular Mixing. Chaos," **9**(3), 611(1999).
Shinbrot, T. and F. J. Muzzio, "Nonequilibrium Patterns in Granular Mixing and Segregation," *Physics Today*, 25 (March) (2000).
Sudah, O., D. Coffing-Beach, et al.. "Quantitative Characterization of Mixing of Free-Flowing Granular Material in Tote (Bin)-Blenders," *Powder Technol*., **126**(2), 191 (2002).
Walton, O. *Mechanics of Granular Materials: New Models and Constitutive Relations*., Elsevier, New York (1983).
Walton, O. R.. "Numerical Simulation of Inclined Chute Flow of Monodisperse," Inelastic, Frictional Spheres," *Mechan. Mater*., **16**:239 (1993).
Walton, O. R., *Numerical Simulation of Inelastic, Frictional Particle-Particle Interactions, Particulate Two-Phase Flow*, M. C. Roco, ed. Boston, Butterworth-Heinemann, pp. 884-911(1993).
Walton, O. R., and R. L. Braun. Viscosity, Granular-Temperature, and Stress Calculations for Shearing Assemblies of Inelastic, Frictional Disks. *J. Rheol*., **50**(5), 949 (1986).
Wightman, C. M. Moahker, et al. Simulation of Flow and Mixing of Particles in a Rotating and Rocking Cylinder. *AIChE J.,* **44**(6), 1266 (1998).
Yanagita, T. "Three-Dimensional Cellular Automaton Model of Segregation of Granular Materials in a Rotating Cylinder," *Physical Review Lett*., **82**(26), 3488 (1999).
Zik, O., D. Levine, et al. "Rotationally Induced Segregation of Granular Materials," *Physical Review Lett*., **73**(5), 644 (1994).

Manuscript received Dec. 17, 2001, revision received May 12, 2004, and final revision received Nov. 23, 2004.